Experimental study of total cross sections for positron and electron scattering by SF_6 molecules

C. Makochekanwa,[1,2] M. Kimura,[1] and O. Sueoka[3]
[1]*Graduate School of Sciences, Kyushu University, Fukuoka 812-8581, Japan*
[2]*Physics Department, Sophia University, Tokyo 102-8554, Japan*
[3]*Graduate School of Science and Engineering, Yamaguchi University, Ube 755-8611, Japan*
(Received 17 April 2004; published 11 August 2004)

The total cross sections (TCSs) for 0.2–1000 eV positrons and for 0.8–1000 eV electrons colliding with SF_6 molecules were measured by a relative method. In the present TCS investigation for electrons, peaks attributed to the a_{1g}, t_{1g}, t_{2g}, and e_g shape resonances identified earlier were observed clearly at 2.2, 7.0, 12.5, and 30 eV. In positron TCSs, a hump centered at about 2.6 eV was observed, followed by a larger and broader peak at around 50 eV. These TCSs are compared with those for C_2F_6 molecules, a hexafluoro molecule showing roughly comparative structures at higher energies than 100 eV, a feature that is attributable to the similarity in molecular size and polarizability. Especially for positron scattering, the TCSs are quite similar to each other over all the energy range investigated. Possible rationales for this similarity are provided.

DOI: 10.1103/PhysRevA.70.022702 PACS number(s): 34.80.Bm, 34.80.Dp, 36.10.Dr

I. INTRODUCTION

The collision of electrons with molecules offers a variety of fundamental processes that have attracted much research attention over the past few decades. These include elastic scattering, ionization, and electronic and rovibrational excitations, in addition to electron attachment. These processes are known to be important in a variety of industrial applications and basic sciences. SF_6 is one of the most essential ingredient gases for extremely efficient electrical insulation. This gas is also used as a source of reactive plasmas for applications ranging from plasma etching of integrated circuits to treatment of biomaterials [1]. However, this molecule is known to have a long lifetime in the atmosphere, causing a serious threat as one of the most notorious global warming potential gases. Hence, concerns over its environmental impact as well as basic applications have renewed the interest in comprehensive studies of this gas [2]. Accordingly, we have undertaken a comparative study of electron and positron scattering from this molecule from a few to a few thousands of eV. By investigating electron and positron scattering comparatively, more details of the underlying physics of the spectroscopy and dynamics are expected to be learnt, and critical evaluation of electron scattering cross sections also becomes possible.

Earlier studies on this molecule include the first absolute total cross section (TCS) measurements for electron impact by Kennerly *et al.* [3] for impact energies 0.5–100 eV, and the subsequent below 1 eV studies by Ferch *et al.* [4], the investigation in the energy range 0.25–25 eV by Romanyuk *et al.* [5], that by Kasperski *et al.* [6] over the energy range 0.5–250 eV, and the higher-energy measurements by Zecca *et al.* [7] for energies 75–4000 eV.

To our knowledge, the only available set of TCSs by both electron and positron impact is that by Dababneh *et al.* [8], although their energy range is limited to the much narrower energy region below 500 eV, compared to the present study where the range is extended to 0.2–1000 eV. These extensions to lower-energy ranges have aided in identifying low-lying resonance scattering phenomena, while those for the higher-energy region were intended for observation of the point of merging of positron and electron TCS phenomena above 600 eV, which was not observable in the limited range of Dababneh *et al.* This merging of the two TCSs is a manifestation of molecular size and geometrical structure effects. In addition, because of the attention we have given to accounting for the effect of forward scattering, which Dababneh *et al.* correctly pointed out as a troublesome source of errors resulting in lower than actual TCS magnitudes, we believe these data go a long way in providing a more accurate positron and electron data set for these molecules. A more comprehensive investigation is still desirable though.

Other relevant studies include those by Christophorou and Olthoff, where they experimentally investigated electron-attachment cross sections and negative ion states of the molecule [9], while Spence and Schulz [10] carried out electron attachment. Dehmer *et al.* [11] and Gianturco *et al.* [12] studied elastic scattering processes theoretically. Phelps and Van Brunt examined and compiled all available cross sections of electron impact, and published a complete set of cross section data for a wide range of energy from 1 meV to 1 keV [13]. On the positron impact side, the only available study is that for differential cross sections by Kauppilla *et al.* [14].

II. EXPERIMENTAL AND THEORETICAL PROCEDURES

A. Experiment

The apparatus used for these TCS measurements for 0.2–1000 eV positrons and 0.4–1000 eV electrons is a linear transmission type time of flight (TOF) instrument with a 600 mm path length. A schematic diagram is shown in Fig. 1. Details about the apparatus can be found in our previous work [15]. Only a brief summary is given here as follows. As a spectrometer for positron and electron beams, a retarding potential unit attached to the TOF apparatus is used for elimination of the contribution from large-energy-loss inelastic scattering and to decrease forward scattered contributions with reduced axial velocities. The retarding potential applied

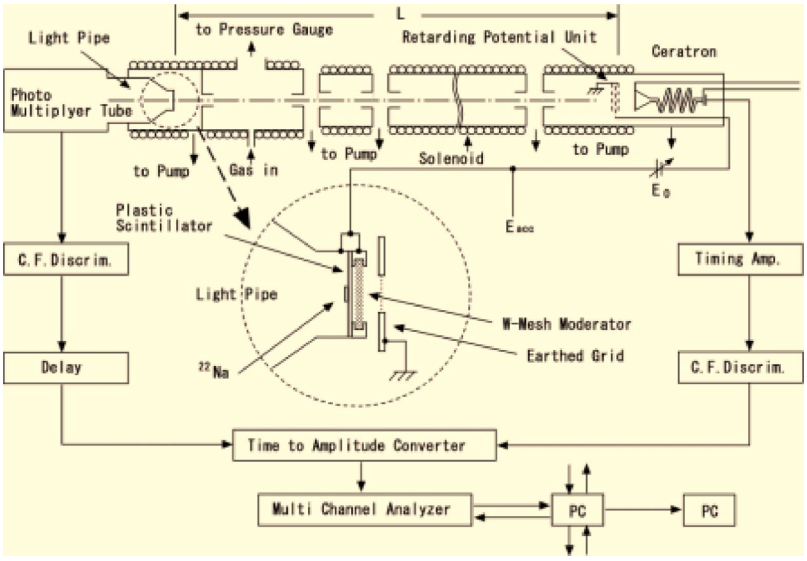

FIG. 1. Schematic diagram of the apparatus and the main electronic circuits. The inset shows the arrangement of the mesh moderator. The abbreviations are as follows: E_{acc}, acceleration potential; E_0, a constant potential; $E_{acc}-E_0$, retarding potential; C.F. Discri., constant fraction discriminator; PC, personal computer.

is the same as the acceleration potential E_{acc} for electron scattering and 1.0 eV lower than E_{acc} for positron scattering.

A ^{22}Na radioisotope with an activity of 90 μCi was used for the positron source. In order to obtain slow positron beams, a set of seven overlapping tungsten meshes baked at 2100 °C was used as the moderator. The energy width of this low-energy positron beam was about 2 eV [full width at half maximum (FWHM)]. The slow electron beam, with an energy width of around 1 eV (FWHM), is composed of secondary electrons produced via multiple scattering from the same tungsten moderator.

In this experiment a magnetic field is used for beam transportation, and also the exit aperture is intentionally made wide, 3 mm in radius, because of the weak positron source. However, this results in an increase in the undesirable forward scattering effects. Hence, a forward scattering correction is necessary to the measured TCS value (Q_{measured}). The relationship between the corrected TCS value (Q_t) and this measured value (Q_{measured}) is given by

$$Q_t = Q_{\text{measured}} + Q_f, \tag{1}$$

where Q_f is the cross section due to forward scattering. The correction method used here was discussed elsewhere [16]. The forward scattering cross section Q_f is given by

$$I_f = \frac{1}{\pi R^2 Q_t}\int_0^{\ell} dI(x)\int_0^{R} 2\pi r dr \times \int_0^{\theta\ \max}\Phi(\theta,r,x,E,B)q(\theta)\sin\theta d\theta, \tag{2}$$

where $q(\theta)$ is the differential cross section (DCS).

In the actual measurements, the TCS values Q_{measured} are given by

$$Q_{\text{measured}} = (-1/nl)\ln(I_g/I_v),$$

where n and l are the gas density in the collision cell and the effective length of the collision cell, respectively. I_g and I_v are the beam intensities in the gas run and the vacuum run, respectively. The lack of dependence of the TCS values on the cell pressure was confirmed using electron collisions, and these data are shown in Fig. 2. As shown in Fig. 2, there is no systematic variation that would indicate the pressure dependence of the TCS.

The errors in the results are the total uncertainties. These total uncertainties were computed from the equation

$$\frac{\Delta Q_t}{Q_t} = \frac{\Delta n}{n} + \frac{\Delta l}{l} + \frac{\Delta I}{I}. \tag{3}$$

The sum of all the uncertainties was estimated to be 4.1–31.4% for positron and 2.6–3.5% for electron impact. These uncertainties are made up of contributions from the below 29% and below 1.2% beam intensities ($\Delta I/I$) for positron and electron impact, respectively, where I refers to $\ln(I_g/I_v)$ above, the contribution from the gas density, $\Delta n/n$, which was below 0.5% for these target molecules, and the contribution due to the determination of the effective length

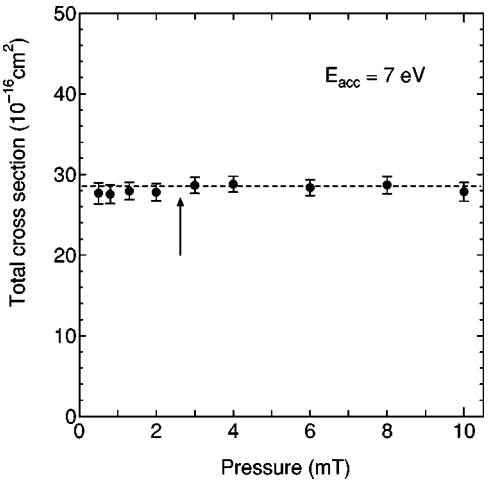

FIG. 2. Electron TCSs for SF_6 plotted against gas pressure for the impact energy 7 eV. The beam intensity attenuation (I_g/I_v) of 1/3, used for the TCS measurement, is shown by arrows. Error bars show the total uncertainties.

of the collision cell, $\Delta l/l$, which was about 2%. The error in the gas density Δn is almost certainly due to the accuracy of the pressure gauge (CMH4-M11, Vacuum General, 0.03 mTorr).

B. Theoretical model

Elastic cross sections (ECSs) are calculated theoretically based on the continuum multiple-scattering (CMS) method, which is a simple but efficient model for treating electron scattering from polyatomic molecules [17] . In order to overcome difficulties arising from (i) the many degrees of freedom of the electronic and nuclear motions and (ii) the nonspherical molecular field in polyatomic molecules, the CMS method uses the technique of dividing the configuration space into three regions: the individual atomic region, the interstitial region, and the outer region surrounding the molecule, respectively. The scattering part of the method is based on the static-exchange-polarization potential model within the fixed-nuclei approximation. The Schrödinger equation in each region is solved numerically under separate boundary conditions, and, by matching the wave functions and their derivatives from each region, we can determine the total wave functions of the scattered electron and hence, the scattering *s* matrix. The scattering cross section can be easily determined by a standard procedure.

III. RESULTS AND DISCUSSION

The TCSs for positron and electron impact were measured using magnetic fields of 9 G and 4.5 G, respectively. As discussed above, these results had to be corrected for the forward scattering effect. This was done using the DCS data of Srivastava *et al.* [18] and Sakae *et al.* [19] for electron scattering. Although positron differential quasielastic scattering cross sections do exist [14], absolute values could not be derived for use in the simulation procedure for the correction of positron TCSs, and hence the same electron DCSs were used for correcting positron impact TCSs as well. Generally speaking, DCSs for electron and positron impact should be quite different, particularly for smaller impact energies below 20 eV or so, but as the energy increases they are expected to become approximately similar. Therefore, we believe that the use of electron DCSs for the positron case may not result in an error greater than 20%. The numerical results for the TCSs for both positron and electron impact are shown in Table I.

A. Electron impact

The present TCSs and ECSs obtained based on the CMS method for electron impact are shown in Figs. 3 and 4, together with the TCS results of Dababneh *et al.* [8], Kasperski *et al.* [6], Kennerly *et al.* [3], and those recommended by NIST[20] and partial cross section data.

1. TCS and ECS results

These results have been partially published elsewhere [21] and so will only be summarized here for the sake of completeness. These results are shown in Fig. 3. The TCS shows a series of resonance peaks at 2.5, 7.0, 12.0, and the broad one at ~30 eV. The ECS result almost shows the same energy dependence as that of the TCS, i.e., the same four resonance peaks, although slightly shifted to higher energies, i.e., at 3, 7, 17, and the change of slope at ~40 eV. These structures should correspond to the a_{1g}, t_{1g}, t_{2g}, and e_g orbital assignments carried out by Dehmer *et al.* [11] in their study of eigenphase sums, where they found fingerprints of these resonances at 2.1, 7.2, 12.7, and 27.0 eV, i.e., in good agreement with our results. Both TCSs and ECSs are seen to decrease above 40 eV. Although the ECS result is included only up to 50 eV, the TCS shows a continued monotonically decreasing trend above 30 eV.

2. Comparisons with other TCSs and partial cross sections

These results are shown in Figs. 4(a) and 4(b). Good qualitative agreement is observed between our TCS results and all the earlier four sets of results shown in Fig 4(a) in that they all show the same resonances, monotonic increase below 1.2 eV, and decrease above 70 eV, as discussed above. However, quantitative differences are observed between our results and those of other measurements, i.e., ours are lower than the other three below 1.2 eV, greater than all at 2–4 eV, and smaller than the other three above 100 eV. At the 7.0, 12.0, and ~30 eV resonance peaks, our result is, respectively, ~3.5% greater, nearly equal to, and ~5% greater than that of Kennerly *et al.* [3], while being less than or equal to the other three measured sets.

TCSs and partial cross sections, The result for this analysis is shown in Fig. 4(b), albeit with only our TCS and that of Christophorou *et al.* [20] (hereafter referred to as the NIST recommended data), which should suffice for this discussion. It is also worth noting here that, although there exists another set of partial cross sections, i.e., for electron attachment, vibration excitation, total ionization, and electronic excitation (data by Phelps *et al.* [13]), the magnitudes and structure agree well with the NIST recommended data [20], and so are not included in Fig. 4(b) to avoid overcrowding the figure. Although good agreement is observed between the present ECSs and the NIST recommended integral elastic cross section result over the energy range of overlap above 3 eV, differences are observed below this energy, with the NIST data producing a minimum at about 1 eV. At this minimum the present ECS is almost two times greater than the NIST result.

Below 2 eV, all TCSs [Fig. 4(a)] decrease to show a minimum at 1.2 eV before rising again, in accordance with the prediction by Dehmer *et al.* [11], who explained the trend as due to an a_{1g} resonance giving rise to sharply increasing cross sections near zero eV. This resonance has been further examined and found to be connected with the formation of a long-lived negative ionic state SF_6^{-*} at near-zero energies [22]. The other groups of data show this trend better in the results of Fig. 4(a), whose lower energies are down to a few meV. That the electron-attachment cross section tends toward the TCS in magnitude in this energy range just reinforces the already established property of these molecules that has made them useful as a dielectric gas, i.e., helping to reduce

TABLE I. Sulfur hexafluoride (SF_6) TCSs (units of 10^{-16} cm^2) for electron and positron scattering.

Energy (eV)	Electron	Positron	Energy (eV)	Electron	Positron
0.2		3.7±1.3	11	29.8±0.8	13.4±0.9
0.4		3.5±1.1	12	31.2±0.9	13.2±1.0
0.6		5.9±1.5	13	30.6±0.9	13.4±1.0
0.8	22.9±0.8	6.4±1.3	14	28.2±0.9	14.1±1.0
1.0	22.3±0.3	7.5±0.6	15	27.2±0.8	14.4±1.0
1.2	21.9±0.6		16	27.1±0.8	14.4±1.0
1.3		9.3±0.7	17	27.5±0.8	14.8±1.0
1.4	22.2±0.6		18	27.5±0.9	14.9±1.1
1.6	22.4±0.7	10.5±0.7	19	27.2±0.9	15.2±1.1
1.8	22.5±0.7		20	27.4±0.9	15.6±1.1
1.9		10.8±0.8	22	27.8±0.8	15.9±1.1
2.0	23.1±0.7		25	28.4±0.9	15.7±1.1
2.2	24.3±0.7	11.0±0.8	30	29.5±0.9	16.8±1.1
2.5	24.7±0.7	11.1±0.8	35	29.1±0.9	
2.8	24.7±0.7	11.4±0.8	40	28.4±0.9	16.7±1.1
3.1	24.5±0.7	11.0±0.8	50	27.4±0.9	17.1±1.1
3.4	24.0±0.7	11.7±0.8	60	26.7±0.9	17.1±1.2
3.7	23.7±0.7	11.2±0.8	70	25.6±0.9	16.3±1.1
4.0	23.1±0.7	11.1±0.8	80	23.9±0.8	15.2±1.1
4.5	22.7±0.6	11.5±0.8	90	23.4±0.8	14.9±1.1
5.0	23.3±0.7	11.8±0.9	100	22.0±0.7	15.1±1.1
5.5	25.9±0.7	12.0±0.9	120	20.7±0.7	14.4±1.2
6.0	27.6±0.8	12.1±0.9	150	18.8±0.6	13.9±1.2
6.5	28.6±0.8	12.5±0.9	200	15.9±0.5	12.8±1.0
7.0	30.8±0.9	12.3±0.9	250	15.2±0.5	12.4±1.1
7.5	30.6±0.9	12.9±0.9	300	14.4±0.5	11.4±1.0
8.0	30.2±0.9	13.0±0.9	400	12.7±0.4	10.2±1.2
8.5	29.8±0.9	12.5±0.9	500	11.0±0.3	9.3±0.9
9.0	29.4±0.9	12.7±0.9	600	9.9±0.3	8.3±0.8
9.5	29.2±0.8	13.2±1.0	800	8.4±0.2	7.2±0.5
10	28.7±0.8	12.8±0.9	1000	7.1±0.2	5.9±0.5

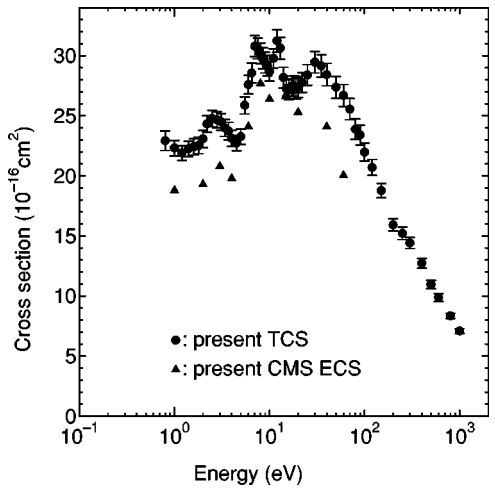

FIG. 3. Present electron impact TCSs (●) and ECSs (CMS ECS) (▲) for SF_6 molecules. Error bars show total uncertainties.

the number of free electrons in a dielectric material through electron attachment at low energies.

It is possibly worth noting here that, in the multichannel contributions to the peaks at 2.5, 7.0, and 12.0 eV, the total vibration excitation channel seems to be the dominant inelastic process, with the conspicuous coincidence of its peaks at 7.0 and 12.0 eV [Fig. 4(b)] with those observed in the TCS. At these peaks, the sums of the ECS and the total vibration excitation are nearly equal to our TCS values at these energies. This does not point to any discrepancies since the next significant inelastic channel is dissociative attachment, which, however, has a very small cross section, i.e., only $\sim 0.05 \times 10^{-16}$ cm^2, at most, in this energy range.

At the energy region above 30 eV, although ionization and neutral dissociation processes become the dominant inelastic channels, with ionization dominating above 40 eV, their contributions to the TCS are still very minimal compared to that due to elastic scattering. For instance, ionization peaks at about 100 eV with a contribution of only 29% to the

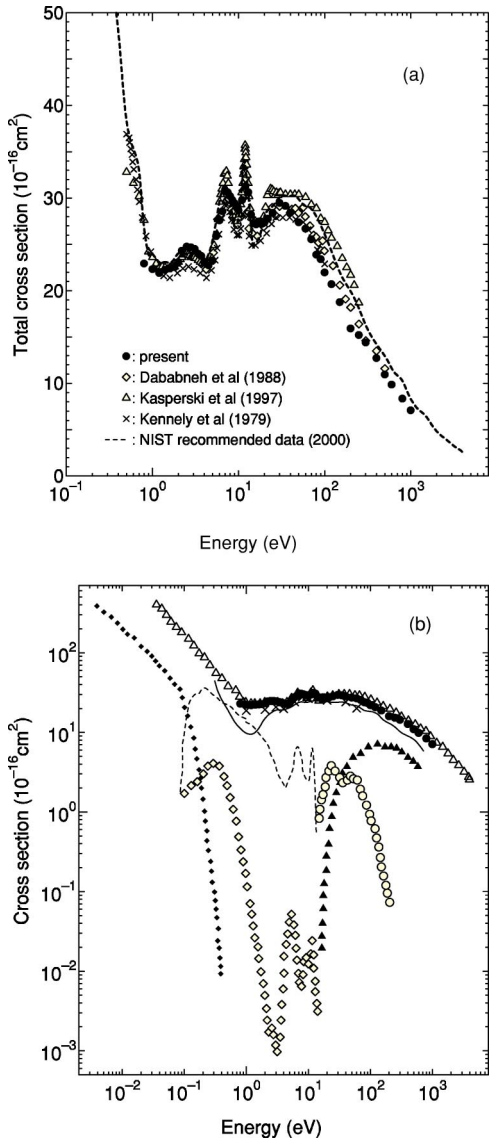

FIG. 4. SF_6 electron scattering: (a) present (●); Dababneh *et al.* [8] (◇); Kasperski *et al.* [6] (△); Kennerly *et al.* [3] (×); NIST recommended (---) [20] TCS results. (b) Present TCS (●); present CMS ECS (×); NIST recommended TCS (△) [20]; total vibration (---); attachment (◆); total ionization (▲); dissociative attachment (◇); elastic integral (—); neutral dissociation (○).

TCS. This, added to its high ionization onset, is yet another desirable property for this gas that has made it useful for gaseous dielectric applications, i.e., this minimal ionization means the gas will not produce many electrons by impact ionization, and hence the number of free electrons will be kept low.

B. Positron impact

The results for the positron impact TCSs are shown in Fig. 5, together with those of Dababneh *et al.* [8]. Our TCSs show a relatively sharp drop below 1.6 eV, although the lowest value at 0.2 eV might be suggesting a turn toward a rise. This drop of the TCSs at these energies might be pointing to

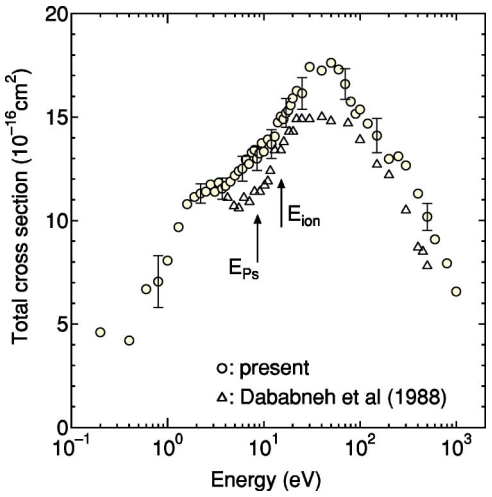

FIG. 5. SF_6 TCSs for positron impact: (○) present result and (△) Dababneh *et al.* [8]. The arrows show the positions of the thresholds for positronium formation, E_{Ps}, and ionization, E_{ion}. Error bars show total uncertainties.

the fact that the attractive and repulsive parts of the interactions accidentally weaken each other in this energy region, hence causing reduced scattering. These TCSs show an unpronounced shoulder centered at about 2.2 eV. Such a distinct structure below the positronium (Ps) formation threshold E_{Ps}, i.e., 8.5 eV, surely needs to be carefully examined to know its origin. It is worth noting here that Kauppila *et al.* [14] too reported similar distinctive structures below E_{Ps} in their DCS studies of these molecules, and speculated that these should indicate less of an absorption effect due to Ps formation. These TCSs rise above 4 eV to produce the main broad peak structure at 20–80 eV. The opening up of the Ps formation channel is not followed by any significant increase in TCSs. This deviates from a trend that we have observed in a systematic study, albeit by an unusual method, of the contribution of this channel to the TCS in the vicinity of E_{Ps} for alkane molecules, whereby they each showed significant increases in TCSs at 2 eV above E_{Ps} [23]. For SF_6, our measurement of the ratio of the cross section for Ps formation, Q_{Ps}, to the TCS at 2 eV above E_{Ps} gave a value of 8.6%, which suggests quite a small contribution to the TCS compared to other molecules studied in our laboratory, especially hydrocarbons.

This smaller contribution from the Ps channel to the TCS means that other inelastic processes, e.g., vibrational and electronic excitation, should be responsible for the increasing TCSs in this energy region. However, as energies increase above this peak region, the TCSs decrease rather monotonically toward 1000 eV, within the limit of experimental errors.

In the comparison of our TCS results with those of Dababneh *et al.* [8], there is general qualitative agreement although significant quantitative differences are observed, whereby our TCSs are greater than their TCSs over the whole energy range of overlap. On the qualitative side, the main difference is at about 5 eV where Ref. [8] report a broad minimum. At this energy, however, our results are still decreasing rather smoothly, although they later slowly turn

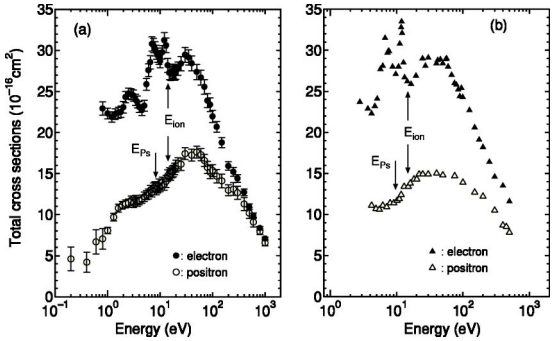

FIG. 6. Total cross sections for electron and positron scattering from SF_6 molecules: (a) electron (●) and positron (○), this work; (b) electron (▲) and positron (△), Dababneh *et al.* [8].

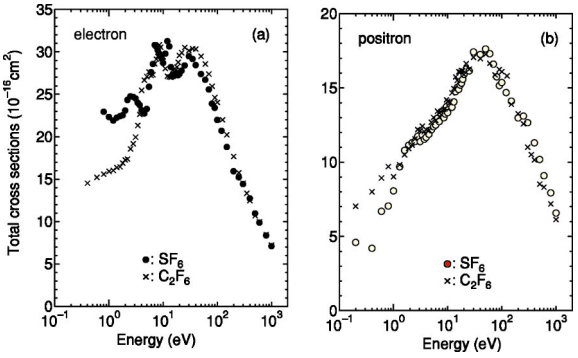

FIG. 7. Total cross sections for (a) electron scattering from (●) SF_6 and (×) C_2F_6 molecules, and (b) positron scattering from (○) SF_6 and (×) C_2F_6 molecules.

over to produce the 2.2 eV structure. The turnover at about 4 eV is rather shallow to be called a minimum. Our TCSs are 16.8% greater than those of Dababneh *et al.* at 5 eV and 14.6% greater at 40 eV, i.e., the center of the main peak. This difference, however, diminishes with increasing impact energies above 80 eV until it becomes 3.1% at 1000 eV.

C. Comparison between electron and positron TCSs

The electron and positron TCSs for these molecules are shown in Figs. 6(a) and 6(b) for our results and those of Dababneh *et al.* [8], respectively. A few interesting features observed from our data are analyzed as follows. At low to intermediate energies, the TCSs for electron impact are larger than the positron TCSs by a factor of more than 2, due to resonances over the region up to 60 eV. These resonances in electron impact are evidenced by the richness in structures of the electron TCSs compared with the rather smoother positron counterparts. This characteristic is a clear reflection of the differences between the interaction schemes for electrons and positrons with the SF_6 molecules. Below 1.2 eV, the electron TCSs show an increasing trend, as discussed earlier, against a background of continually decreasing positron TCSs. This low-energy behavior in the two TCSs is a very sharp contrast. This difference in the two TCSs clearly suggests that the difference in short-range interaction due to the lack of an exchange interaction for the positron significantly contributes to the scattering dynamics, resulting in the different behavior in the two TCSs. The two TCSs, however, approach each other above 500 eV. This should be because, at these higher energies, the long-range interaction alone dominates the scattering event and, as a result, the first Born term alone is sufficient for an accurate description of scattering, where the square of the charge of an incoming particle comes into the cross section formula, leading to this convergence phenomenon in the two sets of TCSs.

The general features of the Dababneh *et al.* electron and positron TCSs agree well with our results, except that their positron TCSs are seen increasing below 2 eV [see Fig. 6(b)]. The other difference is that, whereas our electron and positron TCSs approach each other to within 7.6% at 500 eV, at their highest energy, their electron TCSs are still almost twice as large in magnitude as their positron TCSs. The difference between their electron and positron TCSs in this energy domain appears to be somewhat too large because above a couple of hundred eV the first Born description, which is independent of the charge of the incident particle, is regarded as reasonable, and we have found that most cross sections for electron and positron impact merge within 10% or so. The origin of the difference is not clear yet.

D. SF_6 TCSs compared with C_2F_6 TCSs

Figure 7 shows electron and positron TCSs for SF_6 molecules compared with those for our previously published hexafluroethane (C_2F_6) molecules [27]. It might seem strange to carry out a comparison of these completely different molecules. However, as will be discovered in the discussion to follow, the similarity between the electron TCSs for these molecules above about 15 eV and the positron TCSs over almost all the energy range, is quite interesting and surely deserves attention, although it may be purely accidental.

Although the C_2F_6 electron TCSs do not show all the resonance peaks observed in SF_6 below 15 eV, i.e., they show only two resonance structures at 8.5 eV and 30 eV, these two TCSs show close similarity in structure and magnitude above 15 eV. The difference in their magnitudes in this region decreases from being about 6.6% at 40 eV until they become nearly equal to within 0.5% above 300 eV. The positron TCSs shown in Fig. 7(b) show this similarity even better. Except for the differences in magnitude at 0.6 eV, amounting to ~34%, these TCSs show the same energy dependence over all the rest of the energy range. In addition, they also show a striking similarity in magnitudes, i.e., the difference is on average 5.7% at 1.6–200 eV, before increasing to 12.9% at 300 eV. However, these two TCSs later close in on each other until the difference becomes on average 7.0% at 1000 eV.

That the TCSs for both electron and positron impact for these two molecules become so comparable in size above 100 eV is a feature that might be attributable to the similarity in molecular size (see below), based on the fact that each of these molecules contains six fluorine atoms. Note that the Corey-Pauling-Koltun model [26] has been used to estimate the average diameter of the C_2F_6 molecules.

TABLE II. SF_6 and C_2F_6 molecular properties.

Molecule	Ionization potential[a] (eV)	Polarizability[a] (a.u.)	Valence electron number	Molecular diameter[b] (Å)
SF_6	15.33	6.54	56	5.5
C_2F_6	13.4	6.82	50	5.3

[a]Reference [24].
[b]Reference [25], for SF_6 diameter; Ref. [26] for C_2F_6 diameter.

As compared in Table II, in fact various molecular properties of these two molecules, such as the molecular diameter (5.5 Å for SF_6 vs 5.3 Å for C_2F_6), the number of valence electrons (56 for SF_6 vs 50 for C_2F_6), the ionization potentials, and the polarizabilities, are very close or comparable to each other. In particular, the close values of the polarizability are believed to be responsible for the similarity in the TCSs in the intermediate to higher energy region, while the similar molecular sizes and similar numbers of valence electrons may in some part be reflected in the similarity in size and shape of the TCSs at the lower energy side. Certainly, it may be just a coincidence as we pointed out, but further thorough theoretical and experimental investigations of the strikingly similar shape and magnitude of the two TCSs are warranted.

IV. CONCLUSION

The TCSs for 0.2–1000 eV positron and 0.8–1000 eV electron impact with SF_6 molecules have been experimentally investigated. Electron elastic scattering cross sections for these molecules have also been studied theoretically. In positron TCSs, a hump centered at about 2.6 eV has been observed, followed by a large and broad peak at around 50 eV. No structure has been found that could be associated with the opening up of the Ps formation channel, a feature that seems to point to the fact that the contribution of this channel to the TCS, at least in the vicinity of the Ps formation threshold, is minimal. This is a sharp contrast to our observations in a systematic examination of this channel for alkane molecules. In the TCS data for electrons, peaks attributed to the a_{1g}, t_{1g}, t_{2g}, and e_g resonances studied by Dehmer *et al.* were observed at 2.2, 7.0, 12.5, and 30 eV, respectively. The theoretical elastic cross section is calculated using results from the CMS method, and reproduces reasonably well the general shape, magnitude, and resonance structures of the TCSs by electron impact. These electron cross sections have been found to agree well with other data, for both TCSs and ECSs, available in the literature.

We observe an interesting difference in the low-energy TCSs between electron and positron impact. Below ~2 eV, electron TCSs show an increasing trend, while positron TCSs drop sharply. This difference may be attributable to the role of a short-range interaction. The two TCSs tend toward merging above 600 eV. This might be because at these higher energies the first Born term alone dominates the scattering event.

These TCS data are compared with those from C_2F_6 molecules, a hexafluoro molecule, showing roughly comparative structures at higher energies than 100 eV, a feature that is attributable to the similarity in molecular sizes and polizabilities. This similarity is more pronounced in positron TCSs.

ACKNOWLEDGMENTS

The authors acknowledge Dr. A. Hamada for measurements in the earlier stages of this work. This work was partly supported by the Japan-Germany Collaborative Research Program sponsored by the Japan Society for the Promotion of Science, the Japan Society for Promotion of Science under Grant No. P04064, a Grant-in-Aid by the Ministry of Education, Science, Technology and Culture, Japan, and a Collaborative Research Grant from the National Institute for Fusion Science.

[1] L. G. Christophorouand L. A. Pinnaduwag, IEEE Trans. Electr. Insul. **25**, 55 (1990).
[2] H. Tanaka and O. Sueoka, Adv. At., Mol., Opt. Phys. **44**, 1 (2001). L. G. Christophorou, J. K. Olthoff, and D. S. Green, *Gases for Electrical Insulation and Arc Interruption: Possible Present and Future Alternatives to SF_6*, NIST Technical Note No. 1425 (U.S. GPO, Washington, DC, 1997), pp. 1–44.
[3] R. E. Kennerly, R. A. Bonham, and M. McMillian, J. Chem. Phys. **70**, 2039 (1979).
[4] J. Ferch, W. Raith, and K. Schroder, J. Phys. B **15**, L175 (1982).
[5] H. I. Romanyuk, I. V. Tchernysheva, and O. B. Shpenik, Zh. Tekh. Fiz. **51**, 2051 (1984).
[6] G. Kasperski, P. Mozejko, and C. Szmytkowski, Z. Phys. D: At., Mol. Clusters **42**, 187 (1997).
[7] A. Zecca, G. Karwasz, and R. S. Brusa, Chem. Phys. Lett. **199**, 423 (1992).
[8] M. S. Dababneh, Y.-F. Hsieh, W. E. Kauppila, C. K. Kwan, Steven J. Smith, T. S. Stein, and M. N. Uddin, Phys. Rev. A **38**, 1207 (1988).
[9] L. G. Christophorou and J. K. Olthoff, Int. J. Mass. Spectrom. **205**, 27 (2001).
[10] D. Spence and G. J. Schulz, J. Chem. Phys. **58**, 1800 (1973).
[11] J. Dehmer, J. Siegel and D. Dill, J. Chem. Phys. **69**, 5205

(1978).
[12] F. A. Gianturco, R. R. Lucchese, and N. Sanna, J. Chem. Phys. **102**, 5743 (1995).
[13] A. V. Phelps and R. J. Van Brunt, J. Appl. Phys. **64**, 4269 (1988).
[14] W. E. Kauppila, C. K. Kwan, D. A. Przybyla, and T. S. Stein, Nucl. Instrum. Methods Phys. Res. B **192**, 162 (2002).
[15] O. Sueoka, S. Mori, and A. Hamada, J. Phys. B **27**, 1453 (1994).
[16] A. Hamada and O. Sueoka, J. Phys. B **27**, 5055 (1994).
[17] M. Kimura and H. Sato, Comments At. Mol. Phys. **26**, 333 (1991).
[18] S. K. Srivastava, S. Trajmar, A. Chutjian, and W. Williams, J. Chem. Phys. **64**, 2767 (1976).
[19] T. Sakae, S. Sumiyoshi, E. Mukarami, Y. Matsumoto, K. Ishibashi, and A. Katase, J. Phys. B **22**, 1385 (1989).
[20] L. G. Chrisophorou and J. K. Olthoff, Electron Interactions with SF_6, NIST Ref. Data Ser., http://www.eeel.nist.gov/811/refdata/sf6/cross.htm
[21] C. Makochekanwa, M. Kimura, and O. Sueoka, *Gaseous Dielectrics X* (Kluwer Academic/Plenum Publishers, London, in press).
[22] W. M. Hickam and R. E. Fox, J. Chem. Phys. **25**, 642 (1956).
[23] O. Sueoka, M. K. Kawada, and M. Kimura, Nucl. Instrum. Methods Phys. Res. B **171**, 96 (2000).
[24] *CRC Handbook of Chemistry and Physics*, edited by David R. Lide81st ed. (CRC Press, New York, 2001).
[25] G. Xomeritakis, S. Naik, C. M. Braunbarth, C. J. Cornelius, R. Pardey, and C. J. Brinker, J. Membr. Sci. **215**, 225 (2003).
[26] R. A. Harte, *Molecules in Three Dimensions: A Guide to the Construction of Models of Biologically Interesting Compounds with CPK Models* (American Society of Biological Chemists, Bethesda, MD, 1981), p. 1.
[27] O. Sueoka, C. Makochekanwa, and H. Kawate. Nucl. Instrum. Methods Phys. Res. B **192**, 206 (2002).